J|A|C|S ARTICLES

Published on Web 08/13/2010

Small Molecule-Capped Gold Nanoparticles as Potent Antibacterial Agents That Target Gram-Negative Bacteria

Yuyun Zhao, Yue Tian, Yan Cui, Wenwen Liu, Wanshun Ma, and Xingyu Jiang*

CAS Key Lab for Biological Effects of Nanomaterials and Nanosafety, National Center for NanoScience and Technology, 11 Beiyitiao, ZhongGuanCun, Beijing, China 100190

Received April 6, 2010; E-mail: xingyujiang@nanoctr.cn

Abstract: This report illustrates a new strategy in designing antibacterial agents—a series of commercially available compounds, amino-substituted pyrimidines (themselves completely inactive as antibiotics), when presented on gold nanoparticles (NPs), show antibacterial activities against multidrug-resistant clinical isolates, without external sources of energy such as IR. These pyrimidine-capped gold NPs exert their antibiotic actions via sequestration of magnesium or calcium ions to disrupt the bacterial cell membrane, resulting in leakage of cytoplasmic contents including nucleic acids from compromised cell membranes, and via interaction with DNA and inhibition of protein synthesis by internalized NPs. These amino-substituted pyrimidine-capped gold NPs induce bacterial resistance more slowly compared with conventional, small-molecule antibiotics and appear harmless to human cells; these NPs may hence be useful for clinical applications.

Introduction

Gram-negative bacteria can cause severe infections and have developed unprecedented resistance to drugs, accounting for over two-thirds of the hundreds of thousands of deaths caused by multidrug-resistant (MDR) bacteria in developed economies every year.[1] There are new drugs to treat MDR Gram-positive bacteria but essentially none to treat MDR Gram-negative bacteria.[1,2] New strategies to design antibacterial agents, therefore, are urgently needed. Effective solutions include finding new targets or new mechanisms, such as targeting bacterial lipoproteins,[3] disrupting quorum sensing,[4] or inhibiting bacterial toxins.[5] Our work represents a novel solution that utilizes nontoxic gold nanoparticles (NPs) to activate small-molecule drug precursors.

NPs have been used to improve the remedial efficacy or to fight against MDR bacteria. These applications benefit from one or a few combinations of the properties of NPs: (i) NPs can act as a carrier of drugs to effectively pass through cell membranes.[6−10] (ii) NPs may concentrate drugs on their surfaces to result in polyvalent effects.[5,11−14] (iii) NPs can specifically attack biological targets after modification with target molecules.[15−19] Some materials such as silver are themselves antibacterial; NPs made up of these materials can result in enhanced efficacy.[20−25]

(1) *European Centre for Disease Prevention and Control/European Medicines Agency Joint Technical Report. The bacterial challenge: time to react.* http://www.emea.europa.eu/pdfs/human/ antimicrobial_ resistance/EMEA-576176-2009.pdf.
(2) Levy, S. B.; Marshall, B. *Nat. Med.* **2004**, *10*, S122–S129.
(3) Pathania, R.; Zlitni, S.; Barker, C.; Das, R.; Gerritsma, D. A.; Lebert, J.; Awuah, E.; Melacini, G.; Capretta, F. A.; Brown, E. D. *Nat. Chem. Biol.* **2009**, *5*, 849–856.
(4) Gutierrez, J. A.; Crowder, T.; Rinaldo-Matthis, A.; Ho, M.-C.; Almo, S. C.; Schramm, V. L. *Nat. Chem. Biol.* **2009**, *5*, 251–257.
(5) Kitov, P. I.; Mulvey, G. L.; Griener, T. P.; Lipinski, T.; Solomon, D.; Paszkiewicz, E.; Jacobson, J. M.; Sadowska, J. M.; Suzuki, M.; Yamamura, K.; Armstrong, G. D.; Bundle, D. R. *Proc. Natl. Acad. Sci. U.S.A.* **2008**, *105*, 16837–16842.
(6) Balland, O.; Pinto-Alphandary, H.; Viron, A.; Puvion, E.; Andremont, A.; Couvreur, P. *J. Antimicrob. Chemother.* **1996**, *37*, 105–115.
(7) Rosemary, M. J.; MacLaren, I.; Pradeep, T. *Langmuir* **2006**, *22*, 10125–10129.
(8) Rosi, N. L.; Giljohann, D. A.; Thaxton, C. S.; Lytton-Jean, A. K.; Han, M. S.; Mirkin, C. A. *Science* **2006**, *312*, 1027–1030.
(9) Thomas, M.; Klibanov, A. M. *Proc. Natl. Acad. Sci. U.S.A.* **2003**, *100*, 9138–9143.
(10) Cho, E. C.; Au, L.; Zhang, Q.; Xia, Y. *Small* **2010**, *6*, 517–522.
(11) Bowman, M. C.; Ballard, T. E.; Ackerson, C. J.; Feldheim, D. L.; Margolis, D. M.; Melander, C. *J. Am. Chem. Soc.* **2008**, *130*, 6896–6897.
(12) Gu, H.; Ho, P. L.; Tong, E.; Wang, L.; Xu, B. *Nano Lett.* **2003**, *3*, 1261–1263.
(13) Mammen, M.; Choi, S. K.; Whitesides, G. M. *Angew. Chem., Int. Ed.* **1998**, *37*, 2755–2794.
(14) Yavuz, M. S.; Cheng, Y.; Chen, J.; Cobley, C. M.; Zhang, Q.; Rycenga, M.; Xie, J.; Kim, C. H.; Song, K. H.; Schwartz, A. G.; Wang, L. V.; Xia, Y. *Nat. Mater.* **2009**, *12*, 935–939.
(15) Hyland, R. M.; Beck, P.; Mulvey, G. L.; Kitov, P. I.; Armstrong, G. D. *Infect. Immun.* **2006**, *74*, 5419–5421.
(16) Hyland, R. M.; Griener, T. P.; Mulvey, G. L.; Kitov, P. I.; Srivastava, O. P.; Marcato, P.; Armstrong, G. D. *J. Med. Microbiol.* **2006**, *55*, 669–675.
(17) Lin, C. C.; Yeh, Y. C.; Yang, C. Y.; Chen, C. L.; Chen, G. F.; Chen, C. C.; Wu, Y. C. *J. Am. Chem. Soc.* **2002**, *124*, 3508–3509.
(18) Zharov, V. P.; Mercer, K. E.; Galitovskaya, E. N.; Smeltzer, M. S. *Biophys. J.* **2006**, *90*, 619–627.
(19) Rao, J. *ACS Nano* **2008**, *2*, 1984–1986.
(20) Nair, L. S.; Laurencin, C. T. *J. Biomed. Nanotechnol.* **2007**, *3*, 301–316.
(21) Kumar, A.; Vemula, P. K.; Ajayan, P. M.; John, G. *Nat. Mater.* **2008**, *7*, 236–241.
(22) Loher, S.; Schneider, O. D.; Maienfisch, T.; Bokorny, S.; Stark, W. J. *Small* **2008**, *4*, 824–832.
(23) Huda, S.; Smoukov, S. K.; Nakanishi, H.; Kowalczyk, B.; Bishop, K.; Grzybowski, B. A. *ACS Appl. Mater. Interfaces* **2010**, *2*, 1206–1210.
(24) Sambhy, V.; MacBride, M. M.; Peterson, B. R.; Sen, A. *J. Am. Chem. Soc.* **2006**, *128*, 9798–9808.
(25) Elahifard, M. R.; Rahimnejad, S.; Haghighi, S.; Gholami, M. R. *J. Am. Chem. Soc.* **2007**, *129*, 9552–9553.

Some NPs kill bacteria via photocatalysis[25−27] or photothermal effects.[18,28,29] NPs conjugated with polycations have an enhanced efficacy,[30] but the high toxicity of polymers such as polyethylenimine can limit their application.[9,30] Silver NPs are instable and toxic.[20,31] In contrast to aforementioned NPs, gold NPs are chemically stable, size-controllable, easily modifiable with desired molecules, and nontoxic to mammalian cells or animals.[8,32−34] Several drug-modified gold NPs have been reported, which have pronounced efficacy against MDR bacteria.[6,12,15,16] Some requirements of existing antibiotic NPs might limit their applications; e.g. relying on external sources of energy from focused laser pulses (400−800 nm)[18,28] makes it cumbersome to administer the antibiotic, and relying on existing drugs to modify NPs might not be able to circumvent the development of resistance by bacteria.

In this report, we synthesized antibiotic NPs that are (i) efficacious without external sources of energy, and (ii) modified by small organic molecules that are not drugs themselves.

Many published works show that the resistance of Gram-negative bacteria to most antibiotics arises either from the low permeability of the outer membrane or from the multidrug efflux pump.[35−37] We chose positively charged molecules as ligands of gold NPs to increase the permeability of the outer membrane of bacteria. Multidrug efflux systems can pump out a wide range of small-molecule antibiotics; NPs might comprise a class of poor efflux substrates for efflux pumps because known substrates are all small molecules.[36,37] In addition, presenting potentially active molecules on gold NPs could be an efficient approach to obtaining tethered molecules in multiple copies which may allow the drug to act through the polyvalent effect,[5,11−13] an approach that is more straightforward than many alternatives, such as organic synthesis.[11,12] Another obvious requirement of any antibiotic is that it has to be nontoxic to human cells. On the basis of the above considerations, amino-substituted pyrimidine is a suitable choice as a ligand to modify gold NPs for antibacterial agents. 4,6-Diamino-2-pyrimidinethiol (DAPT), an analogue of 2-pyrimidinethiol that exists in *Escherichia coli* (*E. coli*) *t*RNA, has potential abilities to inhibit the synthesis of *t*RNA.[38−40] DAPT itself, however, has almost no pharmaceutical effect and is often used as a starting compound to develop antibacterial drugs.[39,40] We also investigated antibacterial activities of other positively charged amino-substituted pyrimidines: 4-amino-2-pyrimidinethiol (APT)-capped gold NPs (Au_APT), 2,4-diamino-6-pyrimidinethiol (an isomer of DAPT, iDAPT)-capped gold NPs (Au_iDAPT), and one negatively charged 4,6-dihydroxyl-2-pyrimidinethiol (DHPT)-capped gold NPs (Au_DHPT). We employed laser scanning confocal microscopy (LSCM), transmission electron microscopy (TEM), gel electrophoresis, an *E. coli*-free protein synthesis system, and aggregation assays of NPs to explore antibacterial mechanisms.

Results and Discussion

Synthesis and Characterization of Pyrimidine-Capped Gold NPs. We synthesized pyrimidine-capped gold NPs via reduction of tetrachloroauric acid by sodium borohydride in the presence of the respective pyrimidine ligand in methanol. TEM images and the statistical analysis of diameters of spherical Au_DAPT, Au_APT, Au_iDAPT, and Au_DHPT indicate NPs are around 3 nm (Figure S1 [SI]). UV−vis spectra show the plasma resonance of NPs around 520 nm (Figure S2 [SI]). The UV absorption bands of ligands presented on NPs tend to blue shift, similar to a reported observation,[41] probably induced by the formation of the Au−S bond. X-ray photoelectron spectroscopy (XPS) indicates that the molar ratio of S to Au in Au_DAPT to be 0.45 (XPS, Figure S3 [SI]), that is, the molar ratio of DAPT to Au is 0.45:1, and the number of DAPT per NP is 457 (details of the calculation of the number of molecules on each NP is in the SI). Molar ratios of pyrimidine to Au in respective NPs, numbers of pyrimidine per NP, and surface charges of NPs in water at 25 °C are in Table S1 of SI. Zeta potential values indicate that amino-pyrimidine-capped gold NPs (Au_DAPT, Au_APT, and Au_iDAPT) are positively charged, and hydroxyl-pyrimidine-capped gold NPs (Au_DHPT) are negatively charged. Modified NPs are well-dispersed in aqueous solutions at 4 °C for at least a year.

Antibacterial Activities. We evaluated the antibacterial activities of Au_DAPT or other NPs by determining the optical density at 600 nm ($OD_{600\ nm}$) of bacterial suspension treated with NPs in test tubes for 8 and 24 h (the absorbance of gold NPs is essentially zero compared to that of suspended bacteria at 600 nm). The original bacterial concentration is 1×10^6 colony-forming units (cfu mL^{-1}). An equal volume of water or gentamicin to that of the aqueous solution of NPs is used as a control.

Au_DAPT, Au_APT, and Au_iDAPT can completely inhibit the proliferation of *E. coli* with minimal inhibition concentrations (MICs) of 6 μg mL^{-1} (MIC in molar concentration units in Table S2 [SI]), 8 μg mL^{-1}, and 6 μg mL^{-1} (Figure 1, for concentration effects on each strain, see Figures S4, S5, and S6 [SI]). *Pseudomonas aeruginosa* (*P. aeruginosa*) as a leading pathogenic bacterium has intrinsic resistance to a wide variety of antibiotics mainly because of its exceptionally low permeability of outer membrane and a direct efflux system.[36] MICs of Au_DAPT, Au_APT, and Au_iDAPT for *P. aeruginosa* are 16, 18, and 24 μg mL^{-1}, respectively. Au_DHPT can not inhibit either strain completely at the concentration of 20 μg mL^{-1}, even at 80 μg mL^{-1} (for concentration effects on each strain, see Figure S7 [SI]). At the oversaturation level of 1000 μg mL^{-1}, these molecules themselves alone, DAPT, APT, iDAPT, and DHPT are inactive.

(26) Kubacka, A.; Serrano, C.; Ferrer, M.; Lunsdorf, H.; Bielecki, P.; Cerrada, M. L.; Fernandez-Garcia, M. *Nano Lett.* **2007**, *7*, 2529–2534.
(27) Chen, W. J.; Tsai, P. J.; Chen, Y. C. *Small* **2008**, *4*, 485–491.
(28) Norman, R. S.; Stone, J. W.; Gole, A.; Murphy, C. J.; Sabo-Attwood, T. L. *Nano Lett.* **2008**, *8*, 302–306.
(29) Hu, M.; Chen, J.; Li, Z. Y.; Au, L.; Hartland, G. V.; Li, X.; Marquez, M.; Xia, Y. *Chem. Soc. Rev.* **2006**, *35*, 1084–1094.
(30) Lin, J.; Qiu, S.; Lewis, K.; Klibanov, A. M. *Biotechnol. Prog.* **2002**, *18*, 1082–1086.
(31) Ahamed, M.; Karns, M.; Goodson, M.; Rowe, J.; Hussain, S. M.; Schlager, J. J.; Hong, Y. *Toxicol. Appl. Pharmacol.* **2008**, *233*, 404–410.
(32) Connor, E. E.; Mwamuka, J.; Gole, A.; Murphy, C. J.; Wyatt, M. D. *Small* **2005**, *1*, 325–327.
(33) Esther, R. J.; Bhattacharya, R.; Ruan, M.; Bolander, M. E.; Mukhopadhyay, D.; Sarkar, G.; Mukherjee, P. *J. Biomed. Nanotechnol.* **2005**, *1*, 328–335.
(34) Hainfeld, J. F.; Slatkin, D. N.; Smilowitz, H. M. *Phys. Med. Biol.* **2004**, *49*, 309–315.
(35) Vaara, M. *Microbiol. Rev.* **1992**, *56*, 395–411.
(36) Nikaido, H. *J. Bacteriol.* **1996**, *178*, 5853–5859.
(37) Takatsuka, Y.; Chen, C.; Nikaido, H. *Proc. Natl. Acad. Sci. U.S.A.* **2010**, *107*, 6559–6565.
(38) Carbon, J.; David, H.; Studier, M. H. *Science* **1968**, *161*, 1146–1147.
(39) Sayed, H. H.; Shamroukh, A. H.; Rashad, A. E. *Acta Pharm.* **2006**, *56*, 231–244.
(40) Mostafa, S. I.; Hadjiliadis, N. *Transition Met. Chem.* **2008**, *33*, 529–534.
(41) Zhou, J.; Beattie, D. A.; Ralston, J.; Sedev, R. *Langmuir* **2007**, *23*, 12096–12103.

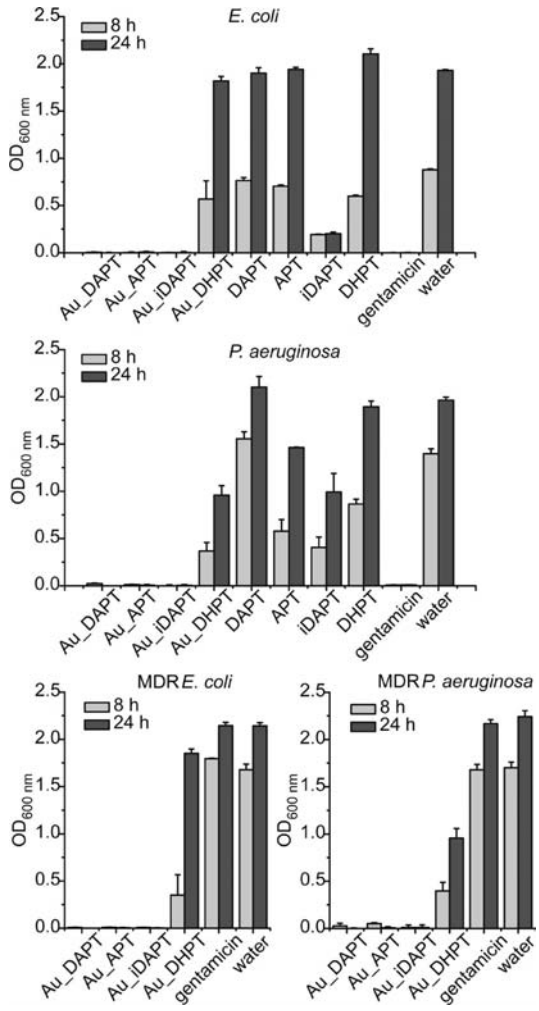

Figure 1. Optical density at 600 nm ($OD_{600\ nm}$) of bacterial suspension treated with various reagents. The original bacterial concentration is 1×10^6 cfu mL^{-1}. For *E. coli*, Au_DAPT: 6 μg mL^{-1} (MIC), Au_APT: 8 μg mL^{-1} (MIC), Au_iDAPT: 6 μg mL^{-1} (MIC), Au_DHPT: 20 μg mL^{-1}, gentamicin: 6 μg mL^{-1}, DAPT, APT, iDAPT, and DHPT alone: 1000 μg mL^{-1}; for *P. aeruginosa*, Au_DAPT: 16 μg mL^{-1} (MIC), Au_APT: 18 μg mL^{-1} (MIC), Au_iDAPT: 24 μg mL^{-1} (MIC), Au_DHPT: 20 μg mL^{-1}, gentamicin: 16 μg mL^{-1}, DAPT, APT, iDAPT, and DHPT alone: 1,000 μg mL^{-1}; for MDR *E. coli*, Au_DAPT: 6 μg mL^{-1} (MIC), Au_APT: 8 μg mL^{-1} (MIC), Au_iDAPT: 6 μg mL^{-1} (MIC), Au_DHPT: 20 μg mL^{-1}, gentamicin: 6 μg mL^{-1}; for MDR *P. aeruginosa*, Au_DAPT: 18 μg mL^{-1} (MIC), Au_APT: 16 μg mL^{-1} (MIC), Au_iDAPT: 32 μg mL^{-1} (MIC), Au_DHPT: 20 μg mL^{-1}, gentamicin: 18 μg mL^{-1}. MICs in molar concentration units are in Table S2 (SI). Each data bar represents the average of three parallel samples, and error bars indicate one standard deviation from the mean.

The antibacterial activities of Au_DAPT on MDR clinical isolates, MDR *E. coli* and MDR *P. aeruginosa*, are particularly striking. Both of these isolates are resistant to at least nine clinically used antibiotics. Au_DAPT, Au_APT, and Au_iDAPT can inhibit the proliferation of MDR bacteria with MICs of 6 μg mL^{-1} (MIC in molar concentration units in Table S2 [SI]), 8 μg mL^{-1}, and 6 μg mL^{-1} for MDR *E. coli*, and 18 μg mL^{-1}, 16 μg mL^{-1}, and 32 μg mL^{-1} for MDR *P. aeruginosa* (Figure 1). The similar MICs of NPs for MDR clinical isolates to that for standard strains suggest that these NPs could probably bypass the resistance mechanisms employed by bacteria to combat conventional, small-molecule antibiotics. Gentamicin is inactive even at a concentration of 100 μg mL^{-1} (for concentration effects, see Figure S8 [SI]). Au_DHPT is less active against bacteria than other NPs, although it can suppress the growth of MDR *E. coli* at the high concentration of 60 μg mL^{-1}.

NP-Induced Disruption of Bacterial Cell Membranes. We explored antibiotic mechanisms of amino-substituted pyrimidine-capped gold NPs with the example of Au_DAPT since it showed the best antibacterial activities among amino-substituted pyrimidine-capped gold NPs. To investigate whether the permeability of cell membranes changed in the presence of Au_DAPT, we treated samples with propidium iodide (PI). PI can bind DNA or RNA specifically to acquire enhanced fluorescence, but it cannot cross the membrane and is excluded from viable cells. Intracellular staining of PI can identify dead cells. After treating suspensions of *E. coli* or *P. aeruginosa* (5.0×10^8 cfu mL^{-1}) with Au_DAPT (the final concentration, 10 μg mL^{-1}) at 37 °C for 4 h and staining them with PI, fluorescence images and statistical analysis show that the permeability of treated bacteria increases (a and b of Figure 2). The percentage of permeable *E. coli* with Au_DAPT is 73% (compared with just 5% in control cells). The percentage of permeable *P. aeruginosa* is 56% (compared with just 14% in control cells. *P. aeruginosa* tends to form biofilms, which include dead bacteria,[42] while *E. coli* does not in our culture conditions). The diffused fluorescence clusters occurring beyond cells imply that some nucleic acids have leaked out of the cells.

We also used TEM to directly visualize the change of membrane morphology and the leakage of nucleic acids. Parts of NP-treated bacteria have broken membranes with an ordered assembly of Au_DAPT aside (Figure 3a and Figure S9 [SI]). To find out if the assembly of NPs might be associated with nucleic acids, we imaged the morphology of λ DNA mixed with Au_DAPT, which formed similar structures in appearance (Figure 3b).

Parts of NP-treated bacteria formed blebs (or outer membrane vesicles, abbreviated as OMVs) while few OMVs formed in untreated cells (c, d, and e of Figure 3, and Figure S9, [SI]). This result is similar to that induced by cationic antibiotics such as polymyxin and gentamicin, which some reports ascribe to the instability of cell membranes.[43,44]

We tested whether Au_DAPT could chelate magnesium ions, as some researchers hypothesize that gentamicin displaces divalent magnesium ions to give rise to OMVs and disrupts bacteria cell membranes which leads to the eventual damage of the bacteria.[35,44] Magnesium ions are essential for the preservation of the structure of ribosomes and the maintenance of permeability barriers of the outer membrane. This fact is supported by assays involving either magnesium starvation[45] or ethylenediaminetetraacetic acid (EDTA) chelation.[35,46] To test the hypothesis that Mg^{2+} depletion may have been one of the ways in which Au_DAPT destroys bacteria, we performed a colorimetric reaction between Au_DAPT and ions to show that Au_DAPT can sequester Mg^{2+}.

We used stably dispersed Au_DAPT in aqueous solutions to test which ions could be sequestered by Au_DAPT. Color changes induced by aggregation of gold NPs are often used to

(42) Webb, J. S.; Thompson, L. S.; James, S.; Charlton, T.; Tolker-Nielsen, T.; Koch, B.; Givskov, M.; Kjelleberg, S. *J. Bacteriol.* **2003**, *185*, 4585–4592.
(43) Vaara, M.; Vaara, T. *Antimicrob. Agents Chemother.* **1983**, *24*, 114–122.
(44) Kadurugamuwa, J. L.; Clarke, A. J.; Beveridge, T. J. *J. Bacteriol.* **1993**, *175*, 5798–5805.
(45) Fiil, A.; Branton, D. *J. Bacteriol.* **1969**, *98*, 1320–1327.
(46) Lusk, J. E.; Williams, R. J. P.; Kennedy, E. P. *J. Biol. Chem.* **1968**, *243*, 2618–2624.

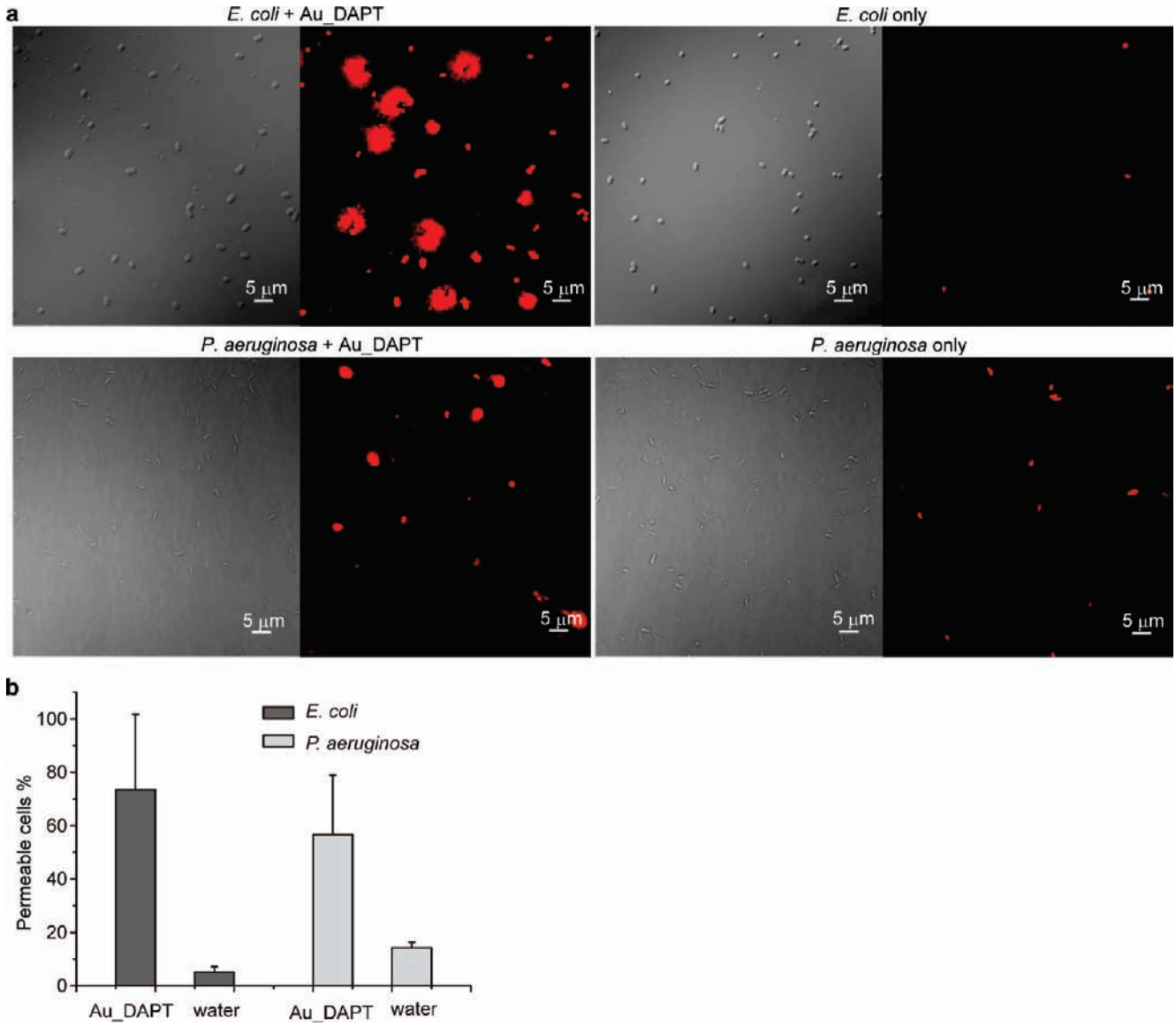

Figure 2. Monitoring NP-induced permeability of cell membranes and leakage of nucleic acids via propidium iodide. (a) For each image, the left half shows an image in the differential interference contrast mode, while the right half shows the corresponding fluorescence image. (b) The percentage of cells with permeable membranes from three or four fields of view from two independent experiments (each field includes 40−100 cells). Error bars indicate standard deviations. P (*E. coli*) = 0.001, P (*P. aeruginosa*) = 0.014.

detect the interaction between molecules because of the dramatic difference in color between dispersed Au NPs (red) and aggregated Au NPs (purple-blue or clear solution with precipitate, reflected by UV−vis spectra as red-shifting, broadening, and decreasing of absorption resonance).[47−49] The colorimetric assay of Au_DAPT with various ions showed that Au_DAPT selectively chelated Mg^{2+} (Figure 3f). Similarly, Au_APT and Au_iDAPT selectively chelated Mg^{2+} (Au_APT also chelated Ca^{2+}), but Au_DHPT did not show the same effect on these ions as the other NPs (Figure S10 [SI]). The corresponding TEM graphs show aggregation of Au_DAPT NPs after exposure to Mg^{2+} (Figure 3g, compared with Figure 3h).

We calculated binding constants, K_{eq}'s between gold NPs and Mg^{2+} via optical absorption titration (details are outlined in the "Binding Constants Calculation" section of SI). With the increase of Mg^{2+}, the absorption resonance of gold NPs red-shifted and decreased. After normalizing absorption curves, there is a linear correlation between the increase in absorbance of NPs at 610 nm and the concentration of Mg^{2+} (0−800 μM). We calculated K_{eq}'s for Au_DAPT, Au_APT, and Au_iDAPT, which are 126 M^{-1}, 133 M^{-1}, and 233 M^{-1}, respectively; these values are similar to those between citric acid and Mg^{2+}. We believe, therefore, Au_DAPT destabilized cell membranes probably by chelating Mg^{2+}, which could also explain increasing permeability of bacteria detected in the fluorescence assay.

We further investigate the effect of Mg^{2+} on antibacterial activities of Au_DAPT by changing the concentration of Mg^{2+}. The concentration of Mg^{2+} is 172 μM in normal nutrient broth. Both high (10 mM) and low (25 μM, this is the lowest we can achieve, and further decrease results in bacterial death) concentrations of Mg^{2+} in the medium can decrease the antibacterial activities of Au_DAPT, whose MIC increased to 2- and 4-fold more than the original MIC against *E. coli*, respectively, similar

(47) De, M.; Ghosh, P. S.; Rotello, V. M. *Adv. Mater.* **2008**, *20*, 1–17.
(48) Zhou, Y.; Wang, S. X.; Zhang, K.; Jiang, X. Y. *Angew. Chem., Int. Ed.* **2008**, *47*, 7454–7456.
(49) Elghanian, R.; Storhoff, J. J.; Mucic, R. C.; Letsinger, R. L.; Mirkin, C. A. *Science* **1997**, *277*, 1078–1081.

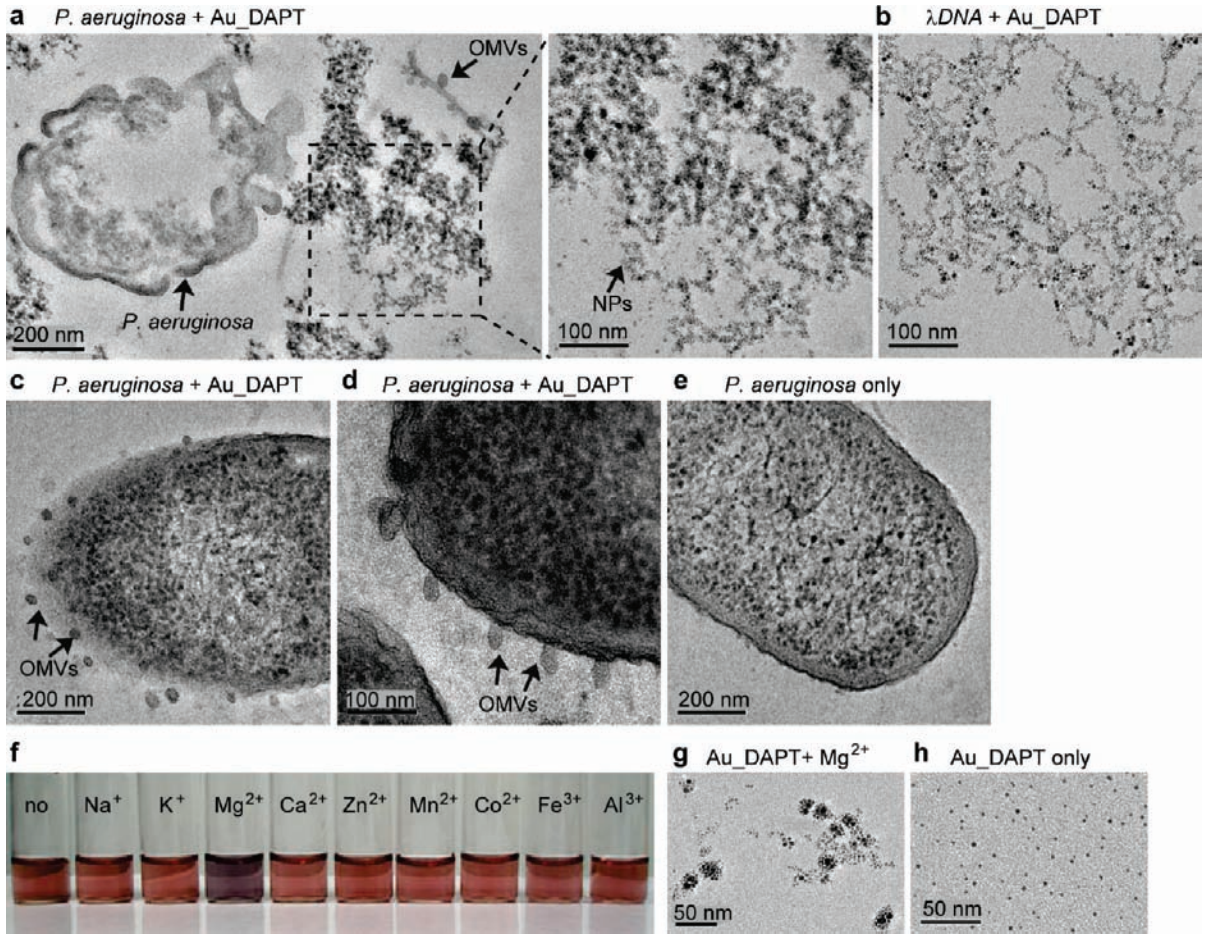

Figure 3. Visualizing NP-induced morphological changes of cell membranes and leakage of nucleic acids via TEM. (a) TEM of stained superthin slices of NP-treated bacteria with a broken cell membrane and magnified view of the area enclosed with a dashed box. (b) TEM of NP-treated λ DNA. (c,d), TEMs of stained superthin slices of NP-treated bacteria with outer membrane vesicles (OMVs). (e) TEM of stained superthin slices of untreated bacteria. (f) A photograph of Mg^{2+}-induced colorimetric assay of Au_DAPT NPs. (g) TEM of Mg^{2+}-induced aggregation of NPs. (h) TEM of well-dispersed Au_DAPT NPs only.

to the effect of changing Mg^{2+} on the action of EDTA, polymyxin, or gentamicin.[43,50,51] These results further suggest that part of the antibacterial effect of Au_DAPT results from changing normal levels of Mg^{2+}.

Interaction between NPs and Subcellular Structures. TEM graphs of unstained superthin slices demonstrate that Au_DAPT NPs can be internalized and located at the outer membrane, peptidoglycan layer, cytoplasmic membrane, and cytoplasm (a and b of Figure 4 and Figure S11 [SI]). TEM graphs of superthin slices stained with 2% uranyl acetate and 0.2% lead citrate can discern the binding of Au_DAPT NPs to the ribosomes and chromosomes (the area with high electron density indicates ribosomes, and the area with low electron density indicates the nucleoid[52,53]), where NPs do not have sufficient contrast from the staining background but can be identified with energy dispersive spectroscopy (EDS, c and d of Figure 4).

Interaction with DNA and Inhibition of Protein Synthesis. Gel electrophoresis reveals that, as the concentration of Au_DAPT increases, more plasmids are retarded, and when the weight ratio of NPs to plasmid is 10:1, the former can completely neutralize the charges of the latter (Figure 5a). Similarly, both Au_APT and Au_iDAPT retard the movement of plasmid as their concentrations increase, completely binding to it at weight ratios of 15:1 and 20:1, respectively. Thus, the binding abilities of NPs to DNA correlate with their antibacterial activities.

To test whether NPs could inhibit protein synthesis, we assayed the expression of the luciferase gene in an *E. coli*-free transcription/translation system with the pBEST*luc* plasmid template in the presence of NPs. The addition of NPs significantly reduces the protein yield (Figure 5b). The IC_{50} values of Au_DAPT, Au_APT, and Au_iDAPT are 13.7, 18.6, and 20.0 μg mL^{-1}, respectively. The highest inhibitory ability of Au_DAPT corresponds to its best antibacterial activities.

Development of Resistance to NPs. Bacteria can almost always evolve strategies for resistance against antibiotics;[2] antibiotics which prevent or retard the emergence of resistance have a favorable prospect for clinical use.[2,54] To investigate the developing rate of bacterial resistance against aminopyrimidine-capped NPs, we exposed a standard strain of *E. coli* (ATCC 11775) to increasing concentrations of Au_DAPT from sub-

(50) Nicas, T. I.; Hancock, R. E. W. *J. Bacteriol.* **1980**, *143*, 872–878.
(51) Macfarlane, E. L. A.; Kwasnicka, A.; Hancock, R. E. W. *Microbiology* **2000**, *146*, 2543–2554.
(52) Someya, A.; Tanaka, K.; Tanaka, N. *Antimicrob. Agents Chemother.* **1979**, *16*, 87–91.
(53) Feng, Q. L.; Wu, J.; Chen, G. Q.; Cui, F. Z.; Kim, T. N.; Kim, J. O. *J. Biomed. Mater. Res.* **2000**, *52*, 662–668.
(54) Davidovich, C.; Bashan, A.; Auerbach-Nevo, T.; Yaggie, R. D.; Gontarek, R. R.; Yonath, A. *Proc. Natl. Acad. Sci. U.S.A.* **2007**, *104*, 4291–4296.

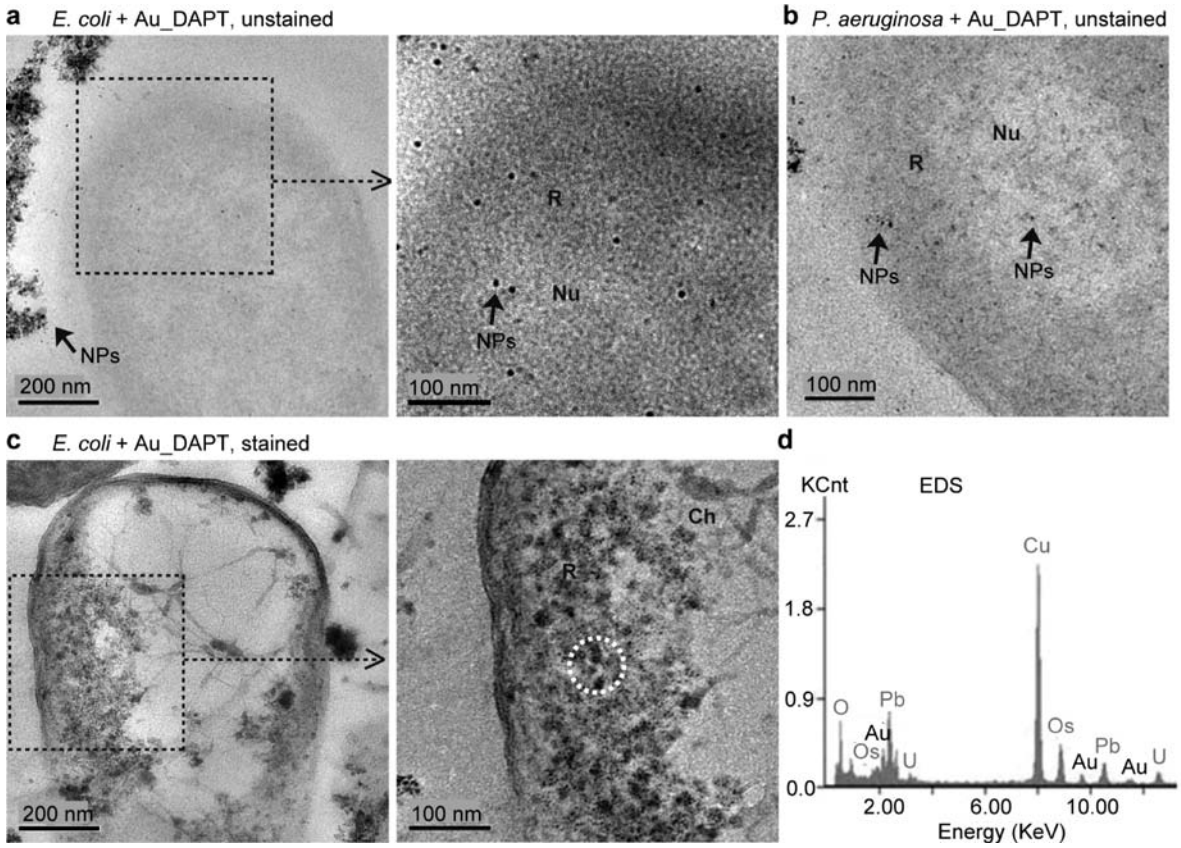

Figure 4. Internalization and location of NPs in bacteria. (a) TEM of unstained superthin slices of *E. coli* with internalized NPs and magnified view of the area enclosed with a dashed box. (b) TEM of unstained superthin slices of *P. aeruginosa* with internalized NPs. (c) TEM of stained superthin slices of *E. coli* and magnified view of the area enclosed with a dashed box indicate that NPs bind to ribosomes. (d) EDS analysis of the area enclosed with a dashed white circle in (c). Nu = nucleoid, R = ribosome, and Ch = chromosome.

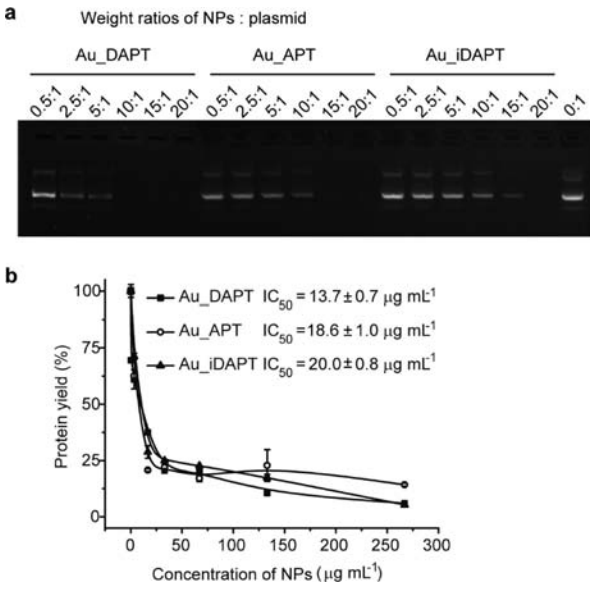

Figure 5. Interaction with DNA and inhibition of protein synthesis. (a) Gel electrophoresis assay of pGFP plasmid in the presence of NPs. (b) Protein synthesis in an *E. coli*-free transcription/translation system in the presence of NPs. IC_{50}'s were calculated by the Spearman−Karber method.

MIC for sustained passages and determined the MIC of NPs for each passage of *E. coli*. After 21 passages in the presence of two-thirds of the MIC of Au_DAPT, bacterial resistance to the original MIC (6 μg mL^{-1}) of NPs emerged, and the MIC increased to 8 μg mL^{-1}. After additional 30 passages of growth in the presence of 6 μg mL^{-1} of NPs (a total of 51 passages), bacterial resistance did not increase any further, and the MIC is still 8 μg mL^{-1}. By contrast, *E. coli* quickly developed resistance to gentamicin, showing resistance to the original MIC (1 μg mL^{-1}) just after one passage and acquiring 10-fold the original MIC (10 μg mL^{-1}) after 10 passages in the presence of increasing concentrations from 2/3 × MIC. This assay indicates that bacteria do not develop significant resistance against pyrimidine-capped gold NPs as easily as they do against small-molecule antibiotics. We believe that compared to small-molecule antibiotics, the reasons why Au_DAPT is less likely to develop resistance may be that the multiple actions of NPs make it difficult for bacteria to simultaneously employ existing strategies for resistance.[55]

Cytotoxicity Assay on Mammalian Cells. A good antibiotic needs to be nontoxic to humans or animals. In order to prepare Au_DAPT for *in vivo* trials, we used primary human cells, human umbilical vein endothelial cells (HUVECs), to test the cytotoxicity of Au_DAPT NPs with a commercial kit (CCK-8 Kit), which can produce soluble purple formazan in the presence of viable cells, and its absorbance increases linearly as cells proliferate. The result shows that Au_DAPT does not affect the viability of HUVECs within the concentration of 100 μg mL^{-1} (Figure 6).

Conclusions

Our report illustrates an antibacterial strategy by presenting pharmaceutically inactive compounds on gold NPs, which act

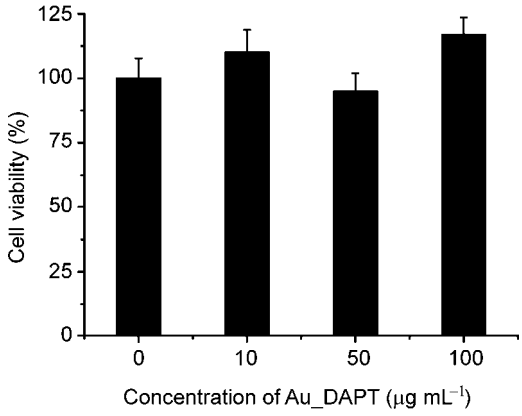

Figure 6. Cytotoxicity assay of Au_DAPT on HUVECs tested by CCK-8 Kit. Each data bar represents an average of six parallels, and error bars indicate one standard deviation from the mean.

on bacteria without employing external sources of energy such as IR. Particularly striking are the abilities of the NPs to target MDR isolates of Gram-negative bacteria, and the slow speed at which bacteria develop resistance against these NPs. These NPs act on bacteria via multiple targets, destabilizing cell membranes, binding to nucleic acids, inhibiting protein synthesis, and inducing the leakage of cytoplasmic contents including nucleic acids. Future work is necessary to elucidate molecular details of interactions between Au_DAPT and bacterial proteins. The nontoxic property of Au_DAPT to primary human cells may facilitate its clinical application. Compared to smal-molecule antibiotics, Au_DAPT may be less likely to develop resistance partly because multiple actions of NPs may not be easily overcome by strategies employed by bacteria to develop resistance simultaneously. In addition, the ease of introduction of different types of reagents onto gold NPs may broaden the molecular space in the search for new antibacterial agents without complex chemical synthesis or sophisticated techniques of separation from the natural environment.

Materials and Methods

$HAuCl_4 \cdot 3H_2O$ (99.99%) was from Shangjuly Chemical Co., Ltd., China. 4,6-Diamino-2-pyrimidinethiol (DAPT) was a gift from Merck China Co., Ltd. 4-Amino-2-pyrimidinethiol (APT), 2,4-diamino-6-pyrimidinethiol (iDAPT), and 4,6-dihydroxyl-2-pyrimidinethiol (DHPT) were from Sigma. Standard strains of *Escherichia coli* (ATCC 11775) and *Pseudomonas aeruginosa* (ATCC 27853) were from China General Microbiological Culture Collection Center. Two clinical isolates, MDR *E. coli* and MDR *P. aeruginosa* were from local hospitals in China. pGFP vector (3.3 kb) was from Clontech Laboratories, Inc. The *E. coli*-free transcription/translation system containing pBEST*luc* vector (4.5 kb) was from Promega (L1020). HUVECs were disassociated from newborns' umbilical cords (Haidian Hospital for Women and Children, Beijing, China). Propidium iodide was from Invitrogen Molecular Probes, Inc. CCK-8 kits were from Beyotime Institute of Biotechnology, China.

Preparation of Pyrimidine-Capped Gold NPs. We stirred the mixture of DAPT (14 mg, 0.1 mmol, dissolved in 10 mL of methanol, 200 μL of absolute acetic acid and 40 mg of Tween 80) and $HAuCl_4 \cdot 3H_2O$ (41 mg, 0.1 mmol, dissolved in 20 mL of methanol) for 10 min in the ice−water bath, added $NaBH_4$ (12 mg, 0.3 mmol, freshly dissolved in 5 mL of methanol) dropwise with vigorous stirring. The solution turned brown immediately and then deep-red. We decreased the stirring speed and kept stirring the solution for another hour in the ice−water bath. We removed methanol in vacuum at 40 °C, added an appropriate volume of deionized water into the residue, dialyzed (14 kDa MW cutoff, Millipore) the solution for 48 h with deionized water, diluted it with water, sterilized it through a 0.22 μm filter (Millipore), and stored it at 4 °C for use. The concentrations of NPs were determined with inductively coupled plasma analysis (ICP, Perkin-Elmer Optima 5300DV). We determined UV−vis absorption of the NPs solution with Varian-Cary Bio100 UV−vis spectrophotometer and ζ potential values with Zetasizer Nano ZS (Malvern Instruments). We centrifuged portions of the stock NPs solution at 9000 rpm through a filter tube (30 kDa MW cutoff, Millipore), washed them with pure water at least three times, and then dried them with a SpeedVac concentrator (Thermo Savant SPD121P, Thermo Scientific) and analyzed elemental contents of the dry powder through XPS using 300 W Al Kα radiation with the base pressure of 3×10^{-9} mbar (ESCALab220i-XL, VG Scientific). Synthesis and characterization of Au_APT, Au_iDAPT, and Au_DHPT are similar to that of Au_DAPT, except no acetic acid was added in the solution of DHPT because acid can induce severe aggregation of Au_DHPT NPs. We calculated the number of gold atoms and ligands per NP using reported methods.[56,57] The detailed calculation and results are described in the Supporting Information.

Determination of Antibacterial Activities of Pyrimidine-Capped Gold NPs. Bacteria were cultured in the nutrient broth medium (5 g L^{-1} NaCl, 10 g L^{-1} tryptone powder, and 5 g L^{-1} beef extract powder, pH = 7.2) at 37 °C on a shaker bed at 200 rpm for 8−10 h and diluted with the broth to a concentration of 1.0×10^8 cfu mL^{-1} (corresponding to an optical density of 0.1 at 600 nm measured with UV−vis spectroscopy). We added 20 μL of each bacterial suspension and 200 μL of each aqueous solution of Au_DAPT, Au_APT, Au_iDAPT, Au_DHPT, DAPT, APT, iDAPT, DHPT, gentamicin, or water into 1.78 mL of broth in test tubes and cultured them at 37 °C on a shaker bed at 200 rpm. We took 100 μL of each mixture after incubation for a certain time into a Corning 96-well plate for the determination of $OD_{600\ nm}$ using Tecan infinite 200 multimode microplate readers and corrected data using UV−vis spectroscopy (Varian-Cary Bio100). We used the broth mixed with Au_DAPT, Au_APT, Au_iDAPT, Au_DHPT, DAPT, APT, iDAPT, DHPT, gentamicin, or water as the blank assay. Cultures were prepared in triplicate, and all experiments were repeated twice or more.

Fluorescence Assay. We cultured 5.0×10^8 cfu mL^{-1} of *E. coli* or *P. aeruginosa* suspension mixed with Au_DAPT at a final concentration of 10 μg mL^{-1} at 37 °C for 4 h on a shaker bed at 200 rpm, collected the suspension by centrifugation at 8000 rpm for 3 min, and washed it with phosphate-buffered saline (PBS, 0.01 M, pH = 7.4) twice. These bacteria were used as fluorescence assay and TEM samples. We incubated the bacterial suspensions with an equal volume of the propidium iodide solution (3 μM in PBS) in the dark for 30 min at room temperature, washed them with PBS twice, and placed 20 μL of samples on a glass slide with a glass coverslip. The control assay was performed without NPs. We observed the fluorescence excited by a 559 nm laser with a laser scanning confocal microscope (Olympus, FV1000-IX81).

Preparation for TEM Samples. We fixed parts of NP-treated bacterial samples for 3 h with 2.5% glutaraldehyde in 0.1 M cacodylate buffer (pH = 7.4), washed them with PBS twice, further fixed the residues with 0.1% osmic acid for 30 min, washed them with PBS for three times, dehydrated the samples through graded ethanol solutions with 30, 50, 70, 90, 95, 100% (v/v, in water), and 50% ethanol in acetone for 10 min each time, and finally dehydrated them with pure acetone twice for 15 min. We embedded the dehydrated samples in Epon812 and polymerized at 60 °C for 24 h. We cut the samples into superthin slices (60−70 nm in thickness) and placed the slices on Formvar-coated grids. Some slices were stained with 2% uranyl acetate and 0.2% lead citrate.

(55) Chopra, I. *J. Antimicrob. Chemother.* **2007**, *59*, 587–590.
(56) Daniel, M.-C.; Ruiz, J.; Nlate, S.; Blais, J.-C.; Astruc, D. *J. Am. Chem. Soc.* **2003**, *125*, 2617–2628.
(57) Leff, D. V.; Ohara, P. C.; Heath, J. R.; Gelbart, W. M. *J. Phys. Chem.* **1995**, *99*, 7036–7041.

We used Tecnai G^2 20 ST TEM from the American FEI company and energy dispersive X-ray spectrometry from American EDAX.

Colorimetric Reaction of Au_DAPT with Ions and Determination of Binding Constants (K_{eq}'s) between Au NPs and Mg^{2+}. We added 75 μL of each ion (2 mM) into 925 μL of Au_DAPT, Au_APT, Au_iDAPT, or Au_DHPT (around 70 μg mL^{-1}), incubated them for around an hour at room temperature and took photographs with an Olympus digital camera (S320). We placed 10 μL of Au_DAPT with or without Mg^{2+} on Formvar-coated copper grids for TEM analysis. We used optical absorption titration curves to determine the binding constants between Au NPs and Mg^{2+}. We added 100 μL of Mg^{2+} (final concentration: 0, 0.05, 0.1, 0.2, 0.4, 0.8, 1.6, 3.2, and 6.4 mM) into 400 μL of Au_DAPT, Au_APT, or Au_iDAPT (70 μg mL^{-1}), incubated them for 2 h at room temperature, and determined UV−vis absorption. The experiment was repeated three times. The details of calculation of binding constants between NPs and Mg^{2+} are in the SI.

The Effects of Mg^{2+} on Antibacterial Activities of Au_DAPT. The concentration of Mg^{2+} in the nutrient broth medium was 172 μM (by ICP). We adjusted Mg^{2+} concentration to 10 mM using $MgSO_4 \cdot 7H_2O$ for experiments involving high Mg^{2+}. The medium with 25 μM of Mg^{2+} was prepared by a mixture of 5 g L^{-1} glucose, 1 g L^{-1} $NH_4H_2PO_4$, 5 g L^{-1} NaCl, 1 g L^{-1} K_2HPO_4, and 6 mg L^{-1} $MgSO_4 \cdot 7H_2O$. *E. coli* cannot grow in the medium without Mg^{2+}. The determination of MIC of Au_DAPT was performed according to the above procedure.

Gel Electrophoresis of Plasmid. We mixed Au_DAPT, Au_APT, or Au_iDAPT with pGFP plasmid at different weight ratios, 0.5:1, 2.5:1, 5:1, 10:1, 15:1, and 20:1, respectively, incubated them at 37 °C for 30 min, placed them on 0.8% agarose gel containing DNA stain (GeneFinder), and performed electrophoresis at 130 V for 30 min. The experiment was repeated twice.

Inhibition Assay of Protein Synthesis. At room temperature, we mixed 1 μg of pBEST*luc* DNA, 1.25 μL of minus leucine, 1.25 μL of minus methionine, 10 μL of S30 Premix without amino acids, 7.5 μL of S30 Extract (circular), and 14 μL of aqueous solution of tested NPs or pure water as a control. We vortexed them for 6 s gently, microcentrifuged them for 6 s, and incubated them at 37 °C for 1 h. We took 12 μL of the reactive mixture into 50 μL of luciferase dilution solution, added 50 μL of room-temperature Luciferase Assay Reagent (Promega), and immediately read the luminescence with Tecan infinite 200 multimode microplate readers. Protein yields were calculated by the ratio of the luminescence in the presence of NPs to that of the control. The assay was performed in duplicate and repeated twice independently.

Induction of Bacterial Resistance by Au_DAPT NPs. We cultured freshly diluted *E. coli* (1.0×10^6 cfu mL^{-1}) in the broth medium in the presence of 4 μg mL^{-1} (2/3 MIC) of Au_DAPT NPs at 37 °C for 12−16 h on a shaker bed at 200 rpm, and tested its sensitivity to 6 μg mL^{-1} (the original MIC) of NPs. After 21 passages, we obtained a strain resistant to 6 μg mL^{-1} of NPs. After further 30 passages in the presence of 6 μg mL^{-1} of NPs, they were susceptible to 8 μg mL^{-1} of NPs. We also induced the resistance of *E. coli* by gentamicin from its 2/3 MIC (0.6 μg mL^{-1}). After one passage, we obtained a strain resistant to its original MIC (1 μg mL^{-1}). After 10 passages in the presence of increasing concentrations of gentamicin, we obtained a strain resistant to 10-fold the original MIC.

Cytotoxicity Assay of Au_DAPT. HUVEC cells were freshly separated from human umbilical vein and cultured in the M199 mixing medium (100 mL of the M199 mixing medium includes 83 mL of Gibco M199, 15 mL of fetal bovine serum, 29.2 mg of glutamine, 10,000 units of penicillin, 10,000 units of streptomycin, and 400 μg of epithelial cell growth factor). We incubated 1×10^4 cells per well of second-generation HUVEC in 96-well plates with 0, 10, 50, 100 μg mL^{-1} of Au_DAPT in 200 μL of M199 medium for 24 h. After discarding the supernatant, we added 10% (v/v) of the CCK-8 solution in M199 and incubated the sample at 37 °C for 4 h. The absorbance at 450 nm (with reference wavelength of 650 nm) was determined by Tecan infinite 200 multimode microplate readers.

Acknowledgment. We thank Ms. Honglan Fu for sample preparation, Prof. Lixin Zhang and Prof. Xingjie Liang for helpful discussions, Merck-China Co. Ltd. for gifts of 4,6-diamino-2-pyrimidinethiol, and Haidian Hospital for Women and Children (Beijing, China) for the supply of newborns' umbilical cords. Funding for this work was provided by the Chinese Academy of Sciences (KJCX2-YW-M15), the National Science Foundation of China (20890020, 90813032), and the Ministry of Science and Technology (2009CB930001, 2006AA03Z323).

Supporting Information Available: TEM graphs of NPs and statistical analysis of their diameters, chemical structures of pyrimidines, UV−vis spectra and XPS of NPs, the calculation of the number of Au atoms and pyrimidines per NP, concentration effects of NPs on inhibition of bacteria, MICs of reagents in molar concentration units, some supporting mechanism research, and the calculation of binding constants between NPs and Mg^{2+}. This material is available free of charge via the Internet at http://pubs.acs.org.

JA1028843